Spring 6-15-2024

Investigating the Role of ebf3a in Craniofacial Development

Shujan A. Sharafeldeen
University of Denver

Investigating the Role of ebf3a in Craniofacial Development

Abstract

Proper craniofacial development requires many genes. Single-cell RNA sequencing (scRNA-seq) allows us to identify genes expressed in precursor cells for craniofacial structures, but the function of many of these genes in craniofacial development has yet to be characterized. In our scRNA-seq of cranial neural crest cells (NCCs), which are precursor cells for the craniofacial skeleton, we found a gene called early B-cell factor 3 (ebf3a) that may be involved in craniofacial development. In our scRNA-seq data, ebf3a expression is restricted to cranial NCCs of the dorsal and ventral domains of pharyngeal arches 1 and 2. In humans, damaging variants in EBF3 are associated with facial dysmorphism. Based on these observations, we hypothesize that ebf3a is an important gene in craniofacial development. In this study, we begin to test this hypothesis by characterizing the expression pattern of ebf3a in cranial NCCs in zebrafish. Through fluorescence in situ hybridization, we confirmed that ebf3a is expressed in the cranial NCCs of the dorsal and ventral patterning domains of pharyngeal arches 1 and 2. This result will be a starting point for future experiments that will investigate the function of ebf3a in craniofacial development.

Document Type

Undergraduate Honors Thesis

Degree Name

B.S in Molecular Biology

First Advisor

Stanley Kanai

Second Advisor

David Clouthier

Third Advisor

Nancy Lorenzon

Keywords

Single-cell RNA sequencing, Cranial neural crest cells (CNCC), Early B-cell factor 3 (ebf3a), Pharyngeal arches, Sanger sequencing, Gel electrophoresis, Colorimetric in situ hybridization (ISH), Fluorescence, Sense probe, Antisense probe, Plasmid, Restriction digest, Embryonic development, Expression pattern, Cell cycle regulator, Pluripotent stem cells (PSCs)

Subject Categories

Dentistry | Genetics and Genomics | Oral Biology and Oral Pathology | Other Dentistry | Other Genetics and Genomics

Investigating the Role of *ebf3a* in Craniofacial Development

Shujan Sharafeldeen

Completed in: University of Colorado School of Dental Medicine

Principal Investigator: Dr. David E. Clouthier

Signature: _____ **Date of signature:** **2/22/24**

Post-Doctoral Fellow: Dr. Stanley M. Kanai

Signature: _____ **Date of signature:** **2/21/24**

12801 E 17th Ave, Aurora, CO 80045

Presented to: University of Denver

2199 S. University Blvd. Denver, CO 80208

ABSTRACT

Proper craniofacial development requires many genes. Single-cell RNA sequencing (scRNA-seq) allows us to identify genes expressed in precursor cells for craniofacial structures, but the function of many of these genes in craniofacial development has yet to be characterized. In our scRNA-seq of cranial neural crest cells (NCCs), which are precursor cells for the craniofacial skeleton, we found a gene called early B-cell factor 3 (*ebf3a)* that may be involved in craniofacial development. In our scRNA-seq data, *ebf3a* expression is restricted to cranial NCCs of the dorsal and ventral domains of pharyngeal arches 1 and 2. In humans, damaging variants in *EBF3* are associated with facial dysmorphism. Based on these observations, we hypothesize that *ebf3a* is an important gene in craniofacial development. In this study, we begin to test this hypothesis by characterizing the expression pattern of *ebf3a* in cranial NCCs in zebrafish. Through fluorescence in situ hybridization, we confirmed that *ebf3a* is expressed in the cranial NCCs of the dorsal and ventral patterning domains of pharyngeal arches 1 and 2. This result will be a starting point for future experiments that will investigate the function of *ebf3a* in craniofacial development.

INTRODUCTION

The head and face are essential for survival for all animals because they house the brain and other vital sensory organs, as well as structures that are essential for eating and breathing (Chai, 2015). For humans, our face determines our identity, our self-esteem, and the way we interact with society. Therefore, the impaired development of our face can lead to neurological and sensory deficits, problems with feeding and breathing, and aesthetic differences that can be a source of social stigma (Volpicelli, 2017; Trainor, 2010). In addition, the cost of service for the affected individual's family can be staggering. Congenital birth differences affecting the face are relatively common, making up 1/3 of all birth defects (Mai, 2019). To better understand the basis of craniofacial differences and care for those who have them, we need to study and comprehend how normal craniofacial development occurs. Our specific goal is to identify genes that play a role in the mechanisms of normal craniofacial development.

Most of the bone and cartilage of the craniofacial skeleton is derived from multipotent cranial neural crest cells (NCCs) (Chai and Maxon, 2006). In pharyngeal arches 1 and 2, cranial NCCs are specified to become specific bone and cartilage elements of the upper and lower jaw structures through tissue patterning (Kanai and Clouthier, 2023). Cranial NCCs are segmented into ventral, intermediate, and dorsal patterning domains by the combinatorial expression patterns of many transcription factors involved in development. Single-cell RNA sequencing (scRNA-seq) is a recently developed technology that allows us to visualize the spatial expression pattern of genes in every cell of a given tissue in an unbiased manner (Tseng and Crump, 2023). ScRNA-seq is a powerful tool that has revealed novel genes that are expressed in cell precursors of craniofacial structures, but the function of many of these genes in craniofacial development remains unknown.

From our scRNA-seq data generated from cranial NCCs of zebrafish at 36 hours post fertilization (hpf) (Figure 1A, B), we hypothesized that *ebf3a* could potentially be involved in patterning of cranial NCCs. The expression of *ebf3a* is restricted to cranial NCCs in the dorsal

and ventral domains (Figure 1C). The expression of *ebf3a* also overlaps with the ventral domain-specific patterning gene *hand2* (Figure 1D) and dorsal domain-specific patterning gene *hey1* (Figure 1E) (Medieros and Crump, 2012). In humans, damaging variants in *EBF3* are associated with facial dysmorphism, in addition to neurological deficits, as well as brain, colorectal, breast, liver, and bone tumors (Zhao et al., 2006; Harms, 2017). Based on these observations, we hypothesize that *ebf3a* in zebrafish plays a role in craniofacial development.

As a first step towards testing this hypothesis, this study characterized the expression pattern of *ebf3a* in a zebrafish embryo. We specifically tested whether the predicted expression pattern of *ebf3a* from our scRNA-sequencing data matches the expression pattern for *ebf3a* in zebrafish embryos using in situ hybridization (ISH) analysis.

MATERIALS AND METHODS

Plasmids

Plasmids for *dlx2a* (Akimenko et al., 1994) and *dlx5a* (Walker et al., 2006) were provided by Dr. James Nichols. The pCRII-*ebf3a* plasmid was generated with the TOPO-TA cloning method following the manufacturer's protocol (ThermoFisher #45-0640). Briefly, a fragment of the *ebf3a* cDNA was amplified using polymerase chain reaction (PCR) and published primer sequences: 5'- atataccgagaggggaacc-3', 5'-acgccgttgctgtacaatag-3' (Li et al., 2010). Primers were purchased as oligonucleotides from Integrated DNA Technologies. PCR was performed with GoTaq DNA polymerase (Promega #M300F). After verifying that the PCR reaction amplified a single product of the expected size (340 bp), the PCR reaction was used in a TOPO-TA cloning reaction (ThermoFisher #450641). The cloning reaction was transformed into TOP10f' competent cells (ThermoFisher #44-0300) and plated on LB agar containing ampicillin, X-gal, and isopropyl β-D-1-thiogalatopyranoside for blue-white screening. White colonies (those with inserts that interrupt the *LacZ* gene, thus preventing expression of β-galactosidase, the enzyme that would otherwise cleave X-gal into a blue color) were picked and grown in liquid culture for plasmid purification. To identify clones containing an insert, plasmids were screened with

restriction digest analysis using EcoRI. Clones that produced a band size of ~340 bp were then analyzed by Sanger sequencing to ensure the identity of the insert.

Synthesis of ISH probes

Digoxigenin (DIG)-labeled ISH probes were synthesized using published methods (Thisse and Thisse, 2007). Briefly, plasmids were linearized with appropriate restriction enzymes and purified by phenol-chloroform extraction. Then, the linear plasmids were used as the template for in vitro transcription using SP6 or T7 RNA polymerase and DIG RNA labeling mix (Roche #11277073910). The sense ISH probe for *ebf3a* was made by digesting the *ebf3a* plasmid with the BamHI enzyme and then transcribing with T7 RNA polymerase. The antisense ISH probe for *ebf3a* was made by digesting the *ebf3a* plasmid with the XhoI enzyme and then transcribing with SP6 RNA polymerase.

Colorimetric and Fluorescence ISH

For both colorimetric and fluorescence ISH, zebrafish embryos were fixed with 4% paraformaldehyde and dehydrated in methanol prior to processing for ISH. Colorimetric ISH was performed on whole-mount zebrafish embryos at 28 hpf following published methods (Thisse and Thisse, 2007). DIG-labeled probes were detected with an anti-DIG-alkaline phosphatase antibody (Roche #11093274910) and color development was performed using 175 µg/ml 5-bromo-4-chloro-3-indoly phosphate (BCIP) and 100 µg/ml nitro-blue tetrazolium (NBT) in alkaline tris buffer (100 mM Tris pH 9.5, 100mM MgCl2, 50 mM NaCl, 0.1% Tween-20). Fluorescence ISH was performed on whole-mount zebrafish embryos containing the *fli1a:EGFP* transgene (Lawson and Weinstein, 2002) at 36 hpf following published methods with slight modifications (Talbot et al., 2010). DIG-labeled RNA probes were detected with anti-DIG-Peroxidase (Roche #11207733910) and fluorescence was applied using the Cy5-Tyramide amplification system (Perkin Elmer #745001). Following the Tyramide amplification step, EGFP was detected using a primary antibody mouse anti-EGFP clone JL-8, (Takara #632381) and a secondary antibody mouse anti-Alexa Fluor 488 (ThermoFisher #A21202).

Imaging

Whole-mount embryos processed for colorimetric ISH were imaged on an Olympus SZX16 microscope using the cellSens Entry software. Whole-mount embryos processed for fluorescence ISH were imaged on a Leica DMI8 microscope equipped with an Andor Dragonfly 301 spinning disk confocal system and Fusion software. Images were processed using Imaris software.

Zebrafish strains and husbandry

All zebrafish (*Danio rerio*) work was approved by the University of Colorado Institutional Animal Care and Use Committee (No. 00188). Zebrafish adults and embryos were raised and staged according to published protocols (Westerfield 2007, Kimmel 1995). Transgenic lines were previously described: *Tg(fli1a:EGFP)*^{y1} (Lawson and Weinstein 2002) and *Tg(sox10:mRFP)*^{vu234} (Kirby et al. 2006). Maintenance of zebrafish lines and collection of live embryos were performed by Dr. Stanley Kanai.

RESULTS

In order to synthesize probes for ISH, we first made a plasmid containing a fragment of *ebf3a* cDNA. We used published primers to amplify a 340 bp region of *ebf3a* coding sequence and then cloned it into a pCRII plasmid. This plasmid is suited for making ISH probes because the cloning site is flanked by promoters for RNA polymerase T7 or SP6, which are used for in vitro transcription of ISH probes. We screened for clones containing the *ebf3a* fragment with a restriction digest assay, and positive clones were subsequently submitted for Sanger sequencing.

The Sanger sequencing result was analyzed using Basic Local Alignment Search Tool (BLAST; National Center for Biotechnology Information), which confirmed that 98% of the plasmid insert aligns with the zebrafish mRNA reference sequence for *ebf3a* (Figure 2). This result indicates we successfully cloned the plasmid for *ebf3a*.

Using the Sanger sequencing result, we verified that the *ebf3a* fragment was incorporated in the plasmid in the 5'-> 3' orientation, which allowed us to choose the correct RNA polymerase promotor to make sense and anti-sense ISH probes. We then linearized the plasmid with restriction enzymes, and the linear plasmids were used for in vitro transcription to make digoxigenin (DIG)-labeled sense and anti-sense ISH probes. 10% of the in vitro transcription reaction was analyzed by gel electrophoresis (Figure 3). We found that the anti-sense reaction produced two bands. One was at ~400 bp and closely matched the predicted size of the fragment. The other was ~500 bp, slightly larger than expected. Seeing two bands following in vitro transcription is a common result. The sense strand was ~400 bp and was close to the predicted size.

We then used the antisense ISH probe against *ebf3a* to perform colorimetric ISH on 28 hpf whole-mount zebrafish embryos, and we also performed ISH with the sense probe as a negative control., We also performed ISH using a probe against *dlx2a* to label the pharyngeal arches (Akimenko,1994). Prominent expression patterns were observed for the antisense probe against *ebf3a* (Figure 4A, B, C), but not the sense probe (Figure 4D, E, F), indicating the specificity of the antisense probe. The expression pattern that we observed for the antisense probe was representative of the 14 embryos that we analyzed. The absence of colorimetric signal for the sense probe was representative of the 10 embryos we analyzed. With the antisense probe, we observed expression in the lateral, dorsal, and ventral regions of the head (Figure 4A, B, C). Specifically, we saw strong signals in the forebrain, midbrain, and hindbrain (Figure 4A, B). However, it was difficult to determine whether *ebf3a* was expressed in the pharyngeal arches given the lack of obvious landmarks. When we compared the expression pattern of *ebf3a* with *dlx2a* (Figure 4 G,H,I), we did not observe an *ebf3a* expression pattern that resembled the pharyngeal arches.

To examine the expression pattern of *ebf3a* in the pharyngeal arches, we performed fluorescence ISH using the antisense probe on 36 hpf whole-mount zebrafish embryos

containing the *fil1a: EGFP* transgene. This transgene labels the vascular and neural crest cell populations in early embryonic development and provides a landmark for the pharyngeal arches (Figure 5). Prominent expression patterns were observed for *ebf3a*, as indicated by the arrows in the ventral regions of pharyngeal arches 1 and 2, and by asterisks in the dorsal regions of pharyngeal arches 1 and 2 (Figure 5).

DISCUSSION

Here, we showed using fluorescence ISH that *ebf3a* is expressed in the ventral and dorsal regions of pharyngeal arches 1 and 2 in 36 hpf zebrafish embryos. This is consistent with the expression pattern of *ebf3a* in our scRNA-sequencing data of cranial NCCs from 36 hpf zebrafish embryos. This provides supporting evidence for our hypothesis that *Ebf3a* is involved in craniofacial development.

A previous study that performed colorimetric ISH on zebrafish embryos reported the expression of *ebf3a* in brain regions but not in the pharyngeal arches (Li et al., 2010). In our colorimetric ISH experiments, we observed similar expression patterns for *ebf3a* in the brain, and although we examined the pharyngeal arches, we could not confidently detect *ebf3a* expression. The inability to detect *ebf3a* in the pharyngeal arches with colorimetric ISH may be because expression in the arch is relatively lower than expression in the brain. The use of fluorescence ISH with the *fli1a: EGFP* transgene, however, allowed us to examine the expression of *ebf3a* in the pharyngeal arches with higher spatial resolution. One limitation of our dataset, however, is that we only tested one time point. To fully characterize the expression pattern of *ebf3a* during the developmental time course that encompasses cranial NCC patterning, follow-up experiments using fluorescence ISH will need to be performed on zebrafish embryos at 18, 24, and 48 hpf.

Now that we have confirmed that *ebf3a* is expressed in the pharyngeal arches, we will next examine its function in the context of craniofacial development. *Ebf3a* is a cell cycle regulator that promotes cell cycle arrest and apoptosis by upregulating the expression of genes involved

in cell cycle arrest such as p21, while simultaneously repressing the expression of genes that are involved in cell proliferation and survival (Zhao, 2006). How would the regulation of cell cycle progression affect NCC patterning? Studies on Pluripotent Stem Cells (PSCs) have shown that the regulation of cell cycle progression plays an essential role in mechanisms of fate determination. PSCs have a unique cell cycle progression with shortened G1 and G2 phases for efficient self-renewal and rapid proliferation. The exposure of PSCs to differentiation signals lengthens the G1 phase and promotes the activation of transcriptional programs that are linked to cell identity (Dalton, 2015). In cranial NCCs, *ebf3a* may be playing a similar role by lengthening G1 and G2 phases to promote the expression of patterning genes.

To test this hypothesis, future studies will examine the relationship between *ebf3a* and cell cycle phases in cranial NCCs. This will be tested by examining the expression of *ebf3a* relative to markers for cell cycle arrest or cell proliferation. For cell cycle arrest, we will use markers including p21. For cell proliferation, we will use Bromodeoxyuridine, which marks cells in S-phase. Based on our hypothesis, we predict that *ebf3a* expression will correlate with markers for cell cycle arrest and not correlate with markers for proliferation.

ACKNOWLEDGEMENTS

I would like to thank Dr. David Clouthier and Dr. Stanley Kanai, for the opportunity to be a part of this project and for helping me throughout my senior thesis. I would also like to thank Dr. James Nichols for providing zebrafish embryos and reagents for the ISH experiments. This work was funded by the National Institute of Dental and Craniofacial Research: F32DE029406 and K99DE032428 to SMK and R01DE029091 to DEC.

REFERENCES

Akimenko MA., Ekker M., Wegner J., Lin W., Westerfield M. 1994. Combinatorial expression of three zebrafish genes related to distal-less: part of a homeobox gene code for the head. The Journal of Neuroscience 14 (6): 3475-86.

Barske L., Askry A., Zuniga E., Balczerski BP., Nichols JT., Crump JC. 2016. Competition between Jagged-Notch and Endothelin1 Signaling Selectivity Restricts Cartilage Formation in the Zebrafish Upper Face. Plos Genetics.

Chai Y., Maxson RE Jr. 2006. Recent advances in craniofacial morphogenesis. Developmental Dynamics 235(9):2353-75.

Chai Y., 2015. Craniofacial Development. 643 pages. Elsevier Science, Netherlands.

Dalton S., 2015. Linking the Cell Cycle to Cell Fate Decisions. Trends in Cell Biology 25(10):592-600.

Harms FL., Girisha KM., Hardigan AA. 2017. Mutations in *EBF3* Disturb Transcriptional Profiles and Cause Intellectual Disability, Ataxia, and Facial Dysmorphism. American Journal of Human Genetics 100(1): 117-127.

Kanai SM., Clouthier DE. 2023. Endothelin signaling in development. Development 15;150(24)

Kimmel CB., Ballard WW., Kimmel SR., Ullmann B., Schilling TF. 1995. Stages of Embryonic Development of the Zebrafish. Developmental Dynamics 203(3)253-310.

Lawson ND., Weinstein BM. 2002. In Vivo Imaging of Embryonic Vascular Development Using Transgenic Zebrafish. Developmental Biology 248(2):307-318.

Li S., Yin M., Liu S., Chen Y., Yin Y., Liu T., Zhou J. 2010. Expression of ventral diencephalon-enriched genes in zebrafish. Developmental Dynamics 239(12): 3368-3379.

Mai CT., Isenburg JL., Canfield AM., Meyer RE., Correa A., Alverson CJ., Lupo PJ., Riehle-Colarusso T., Cho SJ., Aggarwal D., Kirby RS. 2019. National population-based Estimates for Major Birth Defects. Birth Defects Research 1;111(19):1420-1435.

Medeiros DM., Crump JG. 2012. New perspectives on pharyngeal dorsoventral patterning in development and evolution of the vertebrate jaw. Developmental Biology 371(2):121-135.

Talbot JC., Johnson ST., Kimmel. 2010. *hand2* and *dlx* genes specify dorsal, intermediate, and ventral domains within zebrafish pharyngeal arches. Development 137(15): 2507-2517.

Thisse C and Thisse B. 2007. High-resolution *in situ* hybridization to whole-mount zebrafish embryos. Nature protocols 3: 59-69.

Trainor PA., 2010. Craniofacial Birth Defects: The Role of Neural Crest Cells in the Etiology and Pathogenesis of Treacher Collins Syndrome and the Potential for Prevention. American Journal of Medical Genetics 152A:2984-2994.

Tseng KC., Crump JG. 2023. Craniofacial development biology in the single-cell era. Development 150(19): dev202077.

Volpicelli EJ., Pfaff MJ., Hakimi K., Bradley James P., Solem Christian R., Lee Justine C., 2017. Age-Related Differences in Psychosocial Function of Children with Craniofacial Anomalies. Plastic and reconstructive surgery 776-784(9)

Walker MB., Miller CT., Talot JC., Stock DW., Kimmel CB., 2006. Zebrafish *furin* mutants reveal intricacies in regulating Endothelin1 signaling in craniofacial patterning. Developmental Biology 295(1):194-205.

Westerfield M., 2007. The Zebrafish Book. A Guide for the Laboratory Use of Zebrafish (*Danio rerio),* 5th edition. University of Oregon Press, Eugene.

Zhao LY., Niu Y., Santiago A., Liu J., Albert SH., Robertson KD,. Liao D. 2006 Oct 1; An EBF3-mediated transcriptional program that induces cell cycle arrest and apoptosis. Cancer Research 66(19):9445-52.

FIGURES

Figure 1. Predicted expression pattern for *ebf3a* in pharyngeal arches from scRNA-sequencing data.

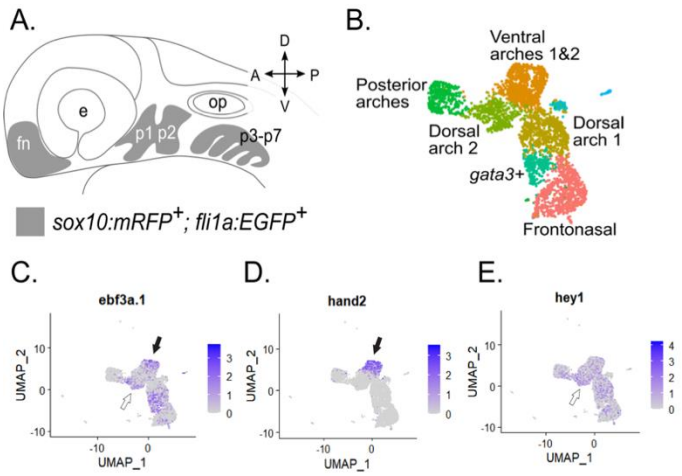

Figure 2. BLAST result of pCRII-*ebf3a*.

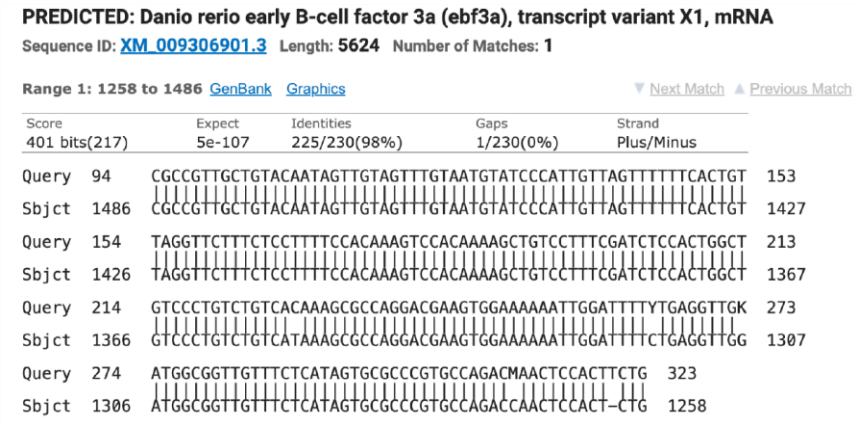

PREDICTED: Danio rerio early B-cell factor 3a (ebf3a), transcript variant X1, mRNA

Sequence ID: XM_009306901.3 Length: 5624 Number of Matches: 1

Range 1: 1258 to 1486 GenBank Graphics ▼ Next Match ▲ Previous Match

Score	Expect	Identities	Gaps	Strand
401 bits(217)	5e-107	225/230(98%)	1/230(0%)	Plus/Minus

```
Query  94    CGCCGTTGCTGTACAATAGTTGTAGTTTGTAATGTATCCCATTGTTAGTTTTTTCACTGT  153
             ||||||||||||||||||||||||||||||||||||||||||||||||||||||||||||
Sbjct  1486  CGCCGTTGCTGTACAATAGTTGTAGTTTGTAATGTATCCCATTGTTAGTTTTTTCACTGT  1427

Query  154   TAGGTTCTTTCTCCTTTTCCACAAAGTCCACAAAAGCTGTCCTTTCGATCTCCACTGGCT  213
             ||||||||||||||||||||||||||||||||||||||||||||||||||||||||||||
Sbjct  1426  TAGGTTCTTTCTCCTTTTCCACAAAGTCCACAAAAGCTGTCCTTTCGATCTCCACTGGCT  1367

Query  214   GTCCCTGTCTGTCACAAAGCGCCAGGACGAAGTGGAAAAAATTGGATTTTYTGAGGTTGK  273
             |||||||||||||| ||||||||||||||||||||||||||||||||| |||||||||
Sbjct  1366  GTCCCTGTCTGTCATAAAGCGCCAGGACGAAGTGGAAAAAATTGGATTTTCTGAGGTTGG  1307

Query  274   ATGGCGGTTGTTTCTCATAGTGCGCCCGTGCCAGACMAACTCCACTTCTG  323
             |||||||||||||||||||||||||||||||||||| ||||||||| |||
Sbjct  1306  ATGGCGGTTGTTTCTCATAGTGCGCCCGTGCCAGACCAACTCCACT-CTG  1258
```

Figure 3. Gel electrophoresis for in vitro transcription of DIG-labeled ISH probes.

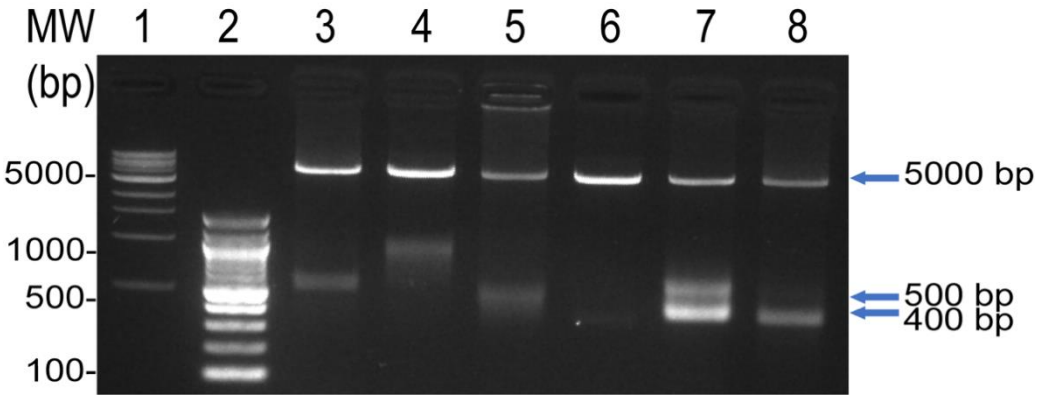

Figure 4. Colorimetric ISH for *ebf3a*.

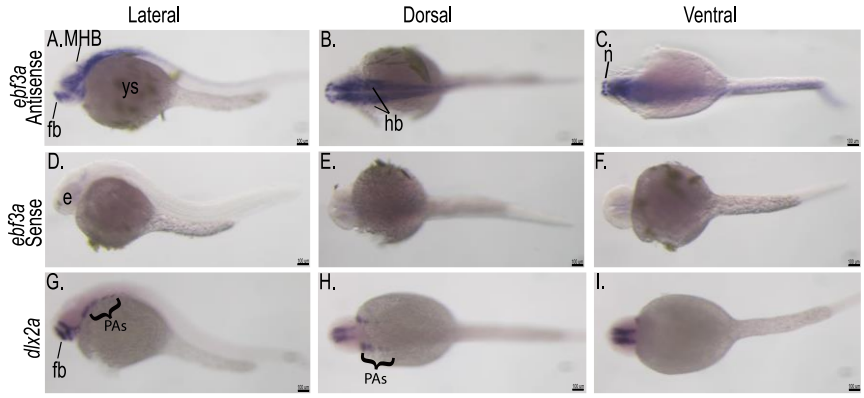

Figure 5. Maximum projection images of whole-mount fluorescence ISH for *ebf3a*.

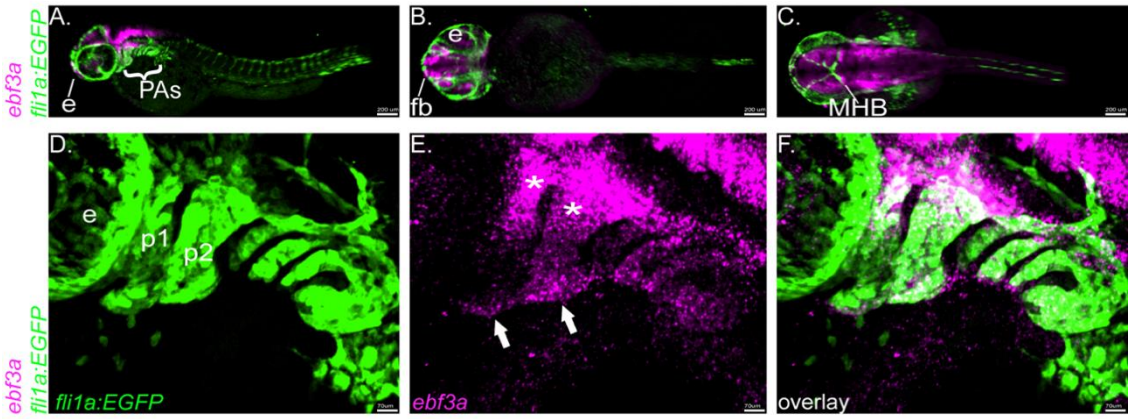

FIGURE LEGENDS

Figure 1. Predicted expression pattern for *ebf3a* in the pharyngeal arches from scRNA-sequencing data. (A) Cartoon of a 36 hpf zebrafish embryo. The *sox10:mRFP* and *fil1a:EGFP* transgenes label the cranial NCC populations (grey) in pharyngeal arches 1 (p1) and 2 (p2), posterior arches (p3-p7), and frontal nasal region (fn). **(B)** UMAP of double-labeled cranial NCCs isolated from 36 hpf embryos, with cluster identities labeled. **(C-E)** Feature plots for pharyngeal arch marker genes. *ebf3a* expression is restricted to the ventral and dorsal clusters, as well as the *gata3*+ cluster, indicated by the black and white arrows (C). *hand2* is highly expressed in the ventral region, indicated by the black arrow (D). *hey1* is a marker for the dorsal region, indicated by the white arrow (E).

Figure 2. BLAST result of pCRII-ebf3a. BLAST search of the pCRII-*ebf3a* sequence (query) aligned with the predicted sequence of *ebf3a* transcript variant X1 (XM_009306901.3; Subject) with 98% match of base pairs.

Figure 3. Gel electrophoresis for in vitro transcription of DIG-labeled ISH probes. Molecular weight ladders are shown in lane 1 (1 kb) and lane 2 (100 bp). The antisense probe for *ebf3a* is shown in lane 7. Products of in vitro transcription were observed at ~500 bp and ~400 bp, as indicated by the arrows. The 5000 bp band represents the linearized plasmid used as a template (indicated by the top arrow). The sense probe for *ebf3a* is shown in lane 8. The product of in vitro transcription was observed at ~400 bp, as indicated by the arrows. The 5000 bp band represents the linearized plasmid used as a template. Lanes 3-6 are in vitro transcription reactions performed for probes not used in this study.

Figure 4. Colorimetric ISH for *ebf3a*. Zebrafish embryos at 28 hpf were processed for colorimetric ISH with antisense probes for ebf3a (A-C), sense probes for *ebf3a* (D-F), or antisense probes for *dlx2a* (G-I). Embryos are shown in lateral (A, D, G), dorsal (B,E,H), and ventral (C,F,I) views. Scale bars in (A-I) are 100 um. Anterior is to the left. e, eye; hb, hindbrain; n, naris; MHB, midbrain-hindbrain boundary; PAs, pharyngeal arches; ys, yolk sack.

Figure 5. Maximum projection images of whole-mount fluorescence ISH. Transgenic zebrafish embryos with *fil1a:EGFP* at 36 hpf were processed with an antisense probe for *ebf3a*. In all images, *fil1a:EGFP* is shown in green, and *ebf3a* is shown in magenta. White indicates the colocalization of *fil1a:EGFP* and *ebf3a*. Images taken with a 10x objective are shown in lateral (A), ventral (B), and dorsal (C) views. An image of the pharyngeal arches taken with a 20x objective, showing *fil1a:EGFP* (D), *ebf3a* I (E), and an overlay (F). In (E), the arrows indicate *ebf3a* expression in the ventral regions of the pharyngeal arches 1 and 2 and the asterisks indicate *ebf3a* expression in the dorsal regions of pharyngeal arches 1 and 2. Scale bars in (A-C) are 200 um. Scale bars in (D-F) is 70 um. Anterior is to the left. e, eye; fb, forebrain; MHB, midbrain-hindbrain boundary; p1, pharyngeal arch 1; p2, pharyngeal arch 2; PAs, pharyngeal arches.